Supporting Information

Construction of Janus particles from single-domain ferroelectric $PbTiO_3$ nanoplates for synergistic photocatalytic H_2 evolution and value-added organic transformation

Yuchen Fang,[a] Chenyang Sun,[a] Xuan Zhan,[a] Zheng Xing,*[a] Gang Liu *[b] and Gangfeng Ouyang *[a]

[a] School of Chemical Engineering and Technology, Sun Yat-sen University, Zhuhai 519082, China

[b] Shenyang National Laboratory for Materials Science, Institute of Metal Research, Chinese Academy of Sciences, Shenyang 110016, China

*Corresponding author. Zheng Xing, xingzh7@mail.sysu.edu.cn; Gang Liu, gangliu@imr.ac.cn; Gangfeng Ouyang, cesoygf@mail.sysu.edu.cn

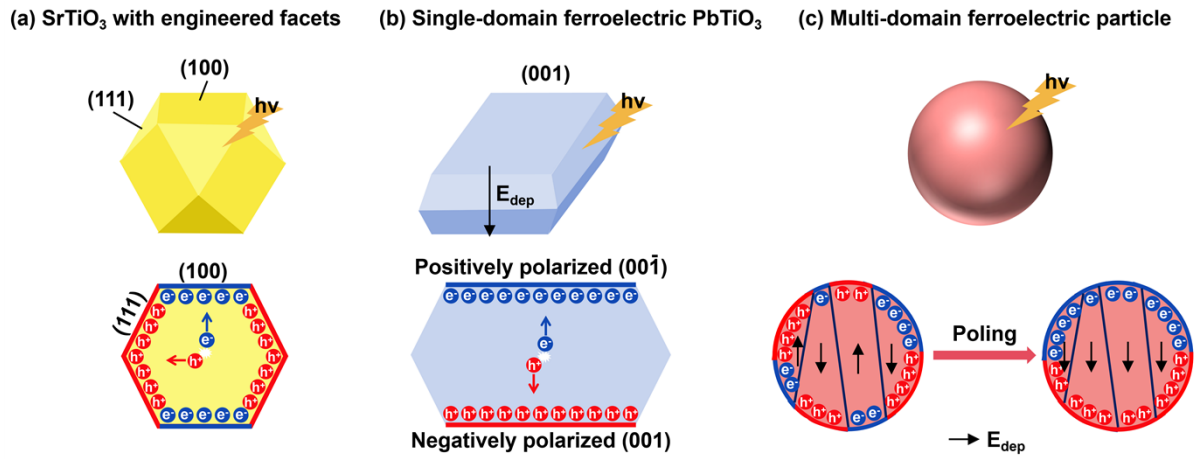

Fig. S1 Schematic illustration of charge separation mechanism within (a) $SrTiO_3$ with engineered facets, (b) single-domain ferroelectric $PbTiO_3$ and (c) multi-domain ferroelectric particle.

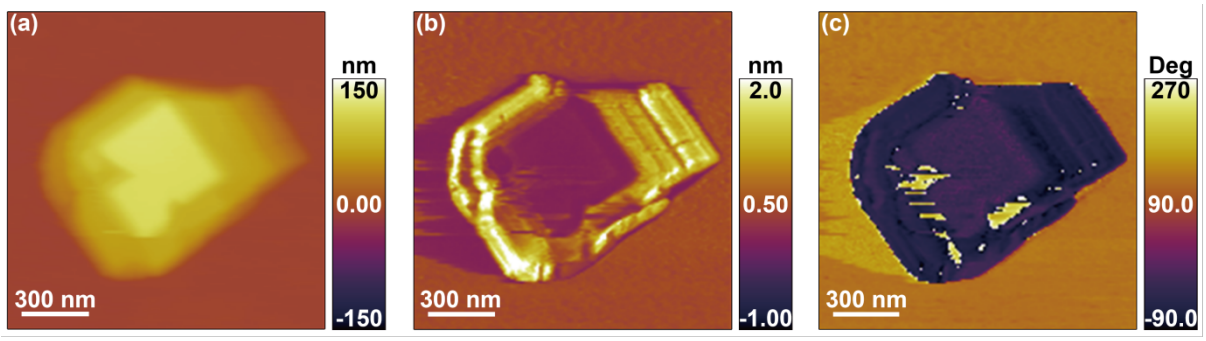

Fig. S2 (a) Topography, (b) amplitude, and (c) phase images of the $PbTiO_3$ nanoplates.

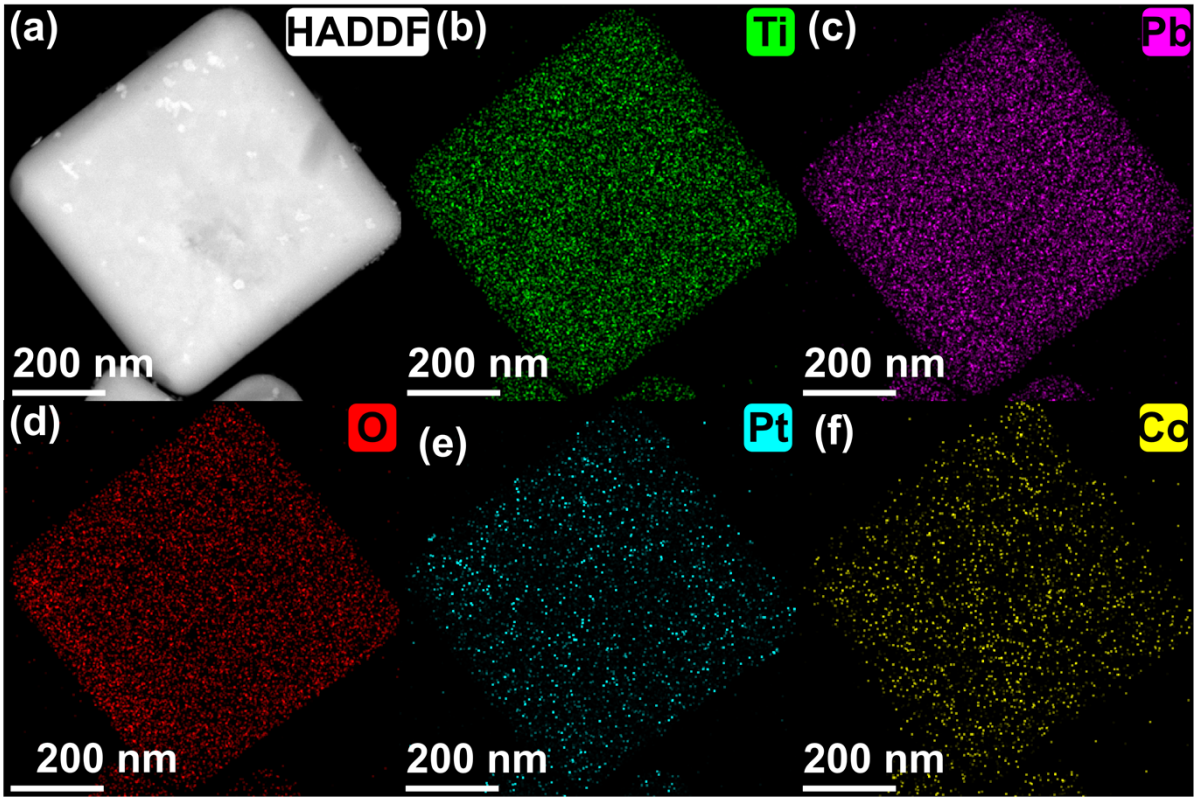

Fig. S3 (a) Top-view HAADF-STEM image and (b-f) corresponding elemental maps of $PbTiO_3$-Pt-CoO_x.

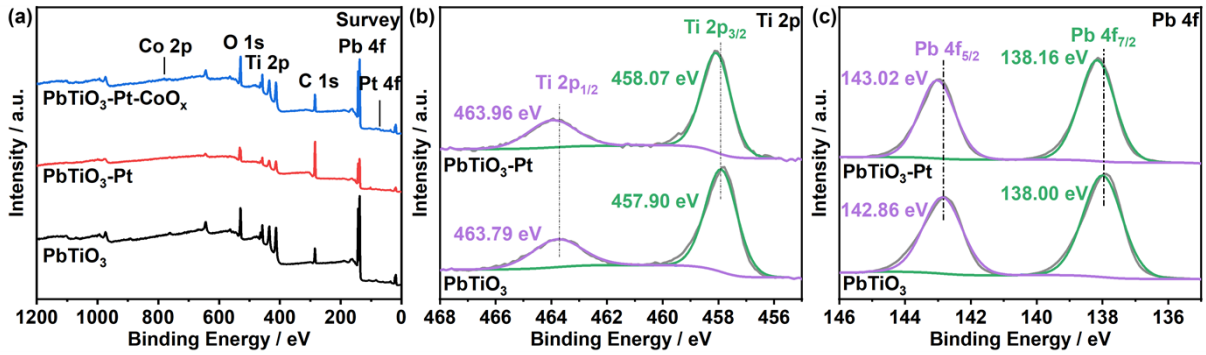

Fig. S4 (a) XPS survey spectra of $PbTiO_3$, $PbTiO_3$-Pt and $PbTiO_3$-Pt-CoO_x. High-resolution XPS spectra of $PbTiO_3$, $PbTiO_3$-Pt-CoO_x for (b) Ti 2p and (c) Pb 4f.

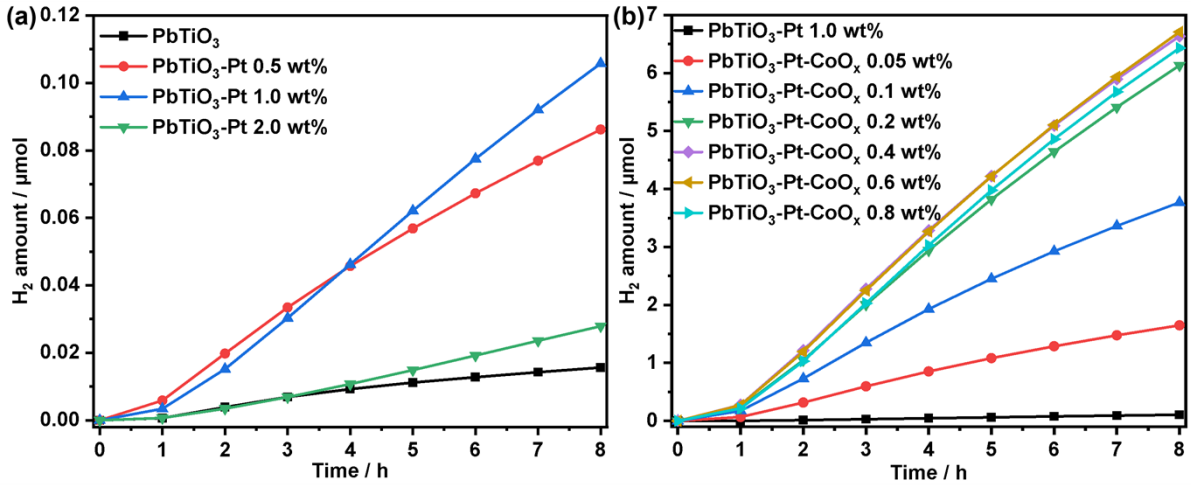

Fig. S5 H_2 generation time profiles of (a) $PbTiO_3$-Pt with different content of Pt and (b) $PbTiO_3$-Pt 1.0 wt%-CoO_x with different amount of CoO_x.

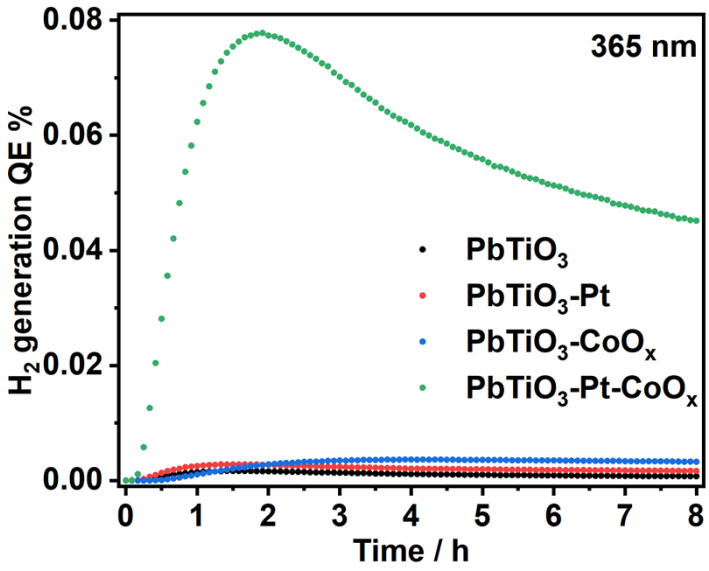

Fig. S6 AQE time profile at 365 nm of $PbTiO_3$, $PbTiO_3$-Pt, $PbTiO_3$-CoO_x and $PbTiO_3$-Pt-CoO_x.

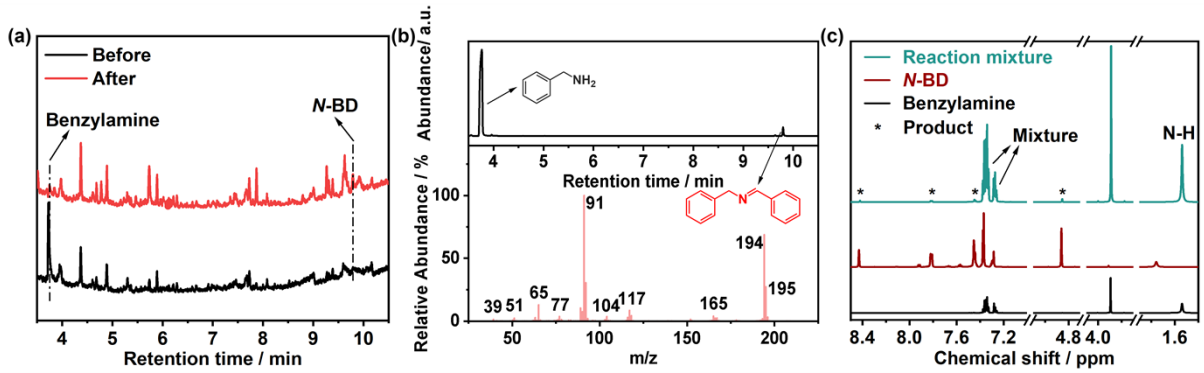

Fig. S7 The main product of BOR was confirmed by gas chromatogram-mass spectrogram (GC-MS) and ^{1}H NMR. (a) The GC traces of reaction mixture before and after photocatalytic reaction at a very low benzylamine concentration (100 μM) with 365 nm LED as the light source. (b) The GC trace (upper) and the corresponding MS spectrum (lower) at the retention time of 9.796 min for the liquid products. The m/z of 195 is in agreement with the theoretical m/z value for N-BD. (c) ^{1}H NMR spectrum of the standard N-BD and benzylamine and the reaction solution after photocatalytic BOR coupled with HER.

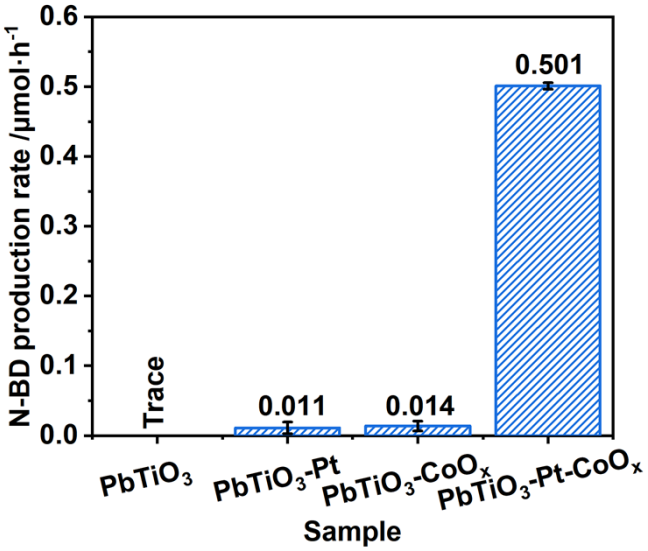

Fig. S8 Average photocatalytic production rates of N-BD using $PbTiO_3$, $PbTiO_3$-Pt, $PbTiO_3$-CoO_x, and $PbTiO_3$-Pt-CoO_x as the catalysts with 200 μL benzylamine.

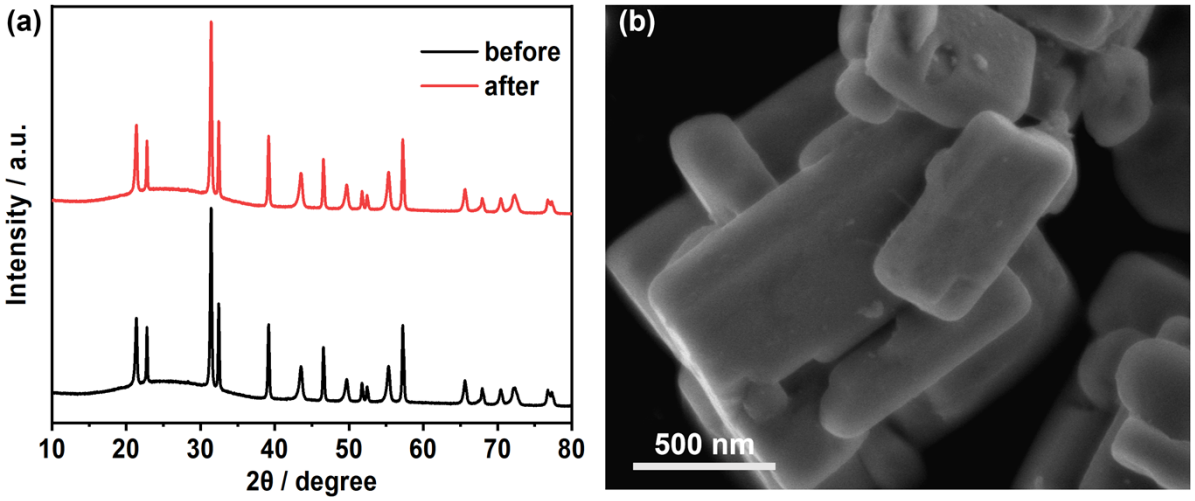

Fig. S9 (a) XRD patterns of $PbTiO_3$-Pt-CoO_x before and after the reusability test. (b) The SEM image of $PbTiO_3$-Pt-CoO_x after the reaction.

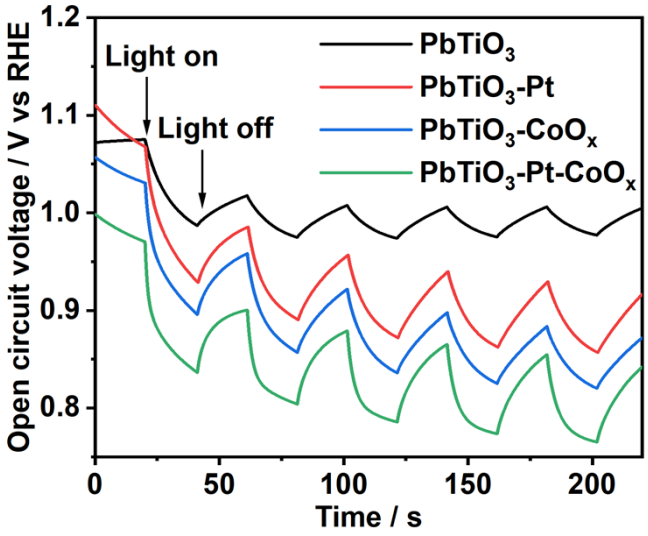

Fig. S10 OCV response to light on/off of $PbTiO_3$, $PbTiO_3$-Pt, $PbTiO_3$-CoO_x and $PbTiO_3$-Pt-CoO_x measured in the 0.5 M Na_2SO_4 and 0.1 M benzylamine mixed aqueous solution.

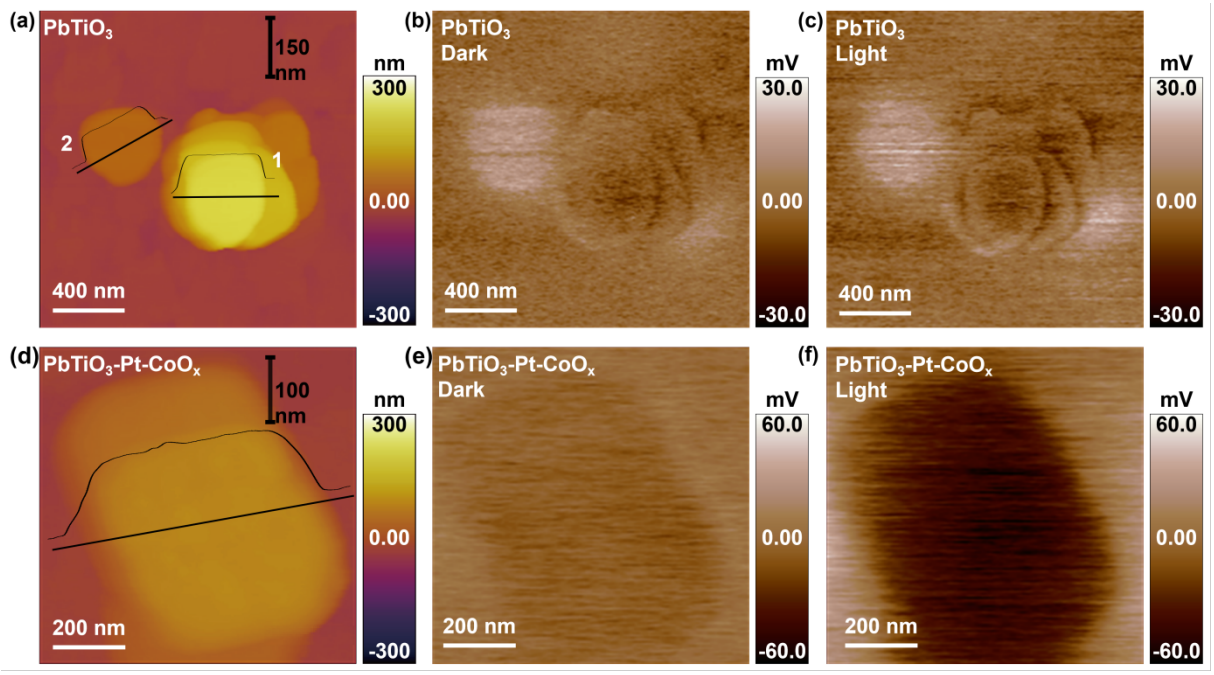

Fig. S11 AFM and spatially distribution of CPD signals in the dark and under illumination of (a-c) $PbTiO_3$ and (d-e) $PbTiO_3$-Pt-CoO_x.

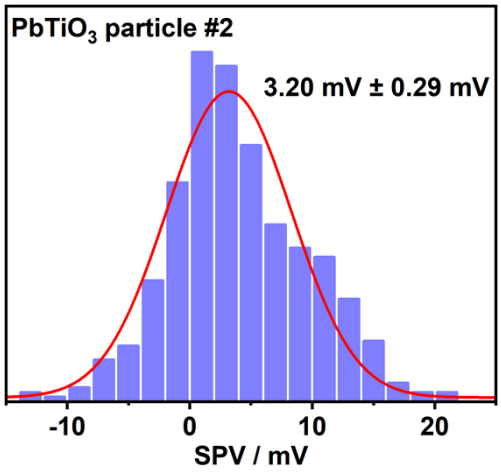

Fig. S12 SPV distribution of $PbTiO_3$ particle #2 obtained from the sample areas of the SPV image of $PbTiO_3$.

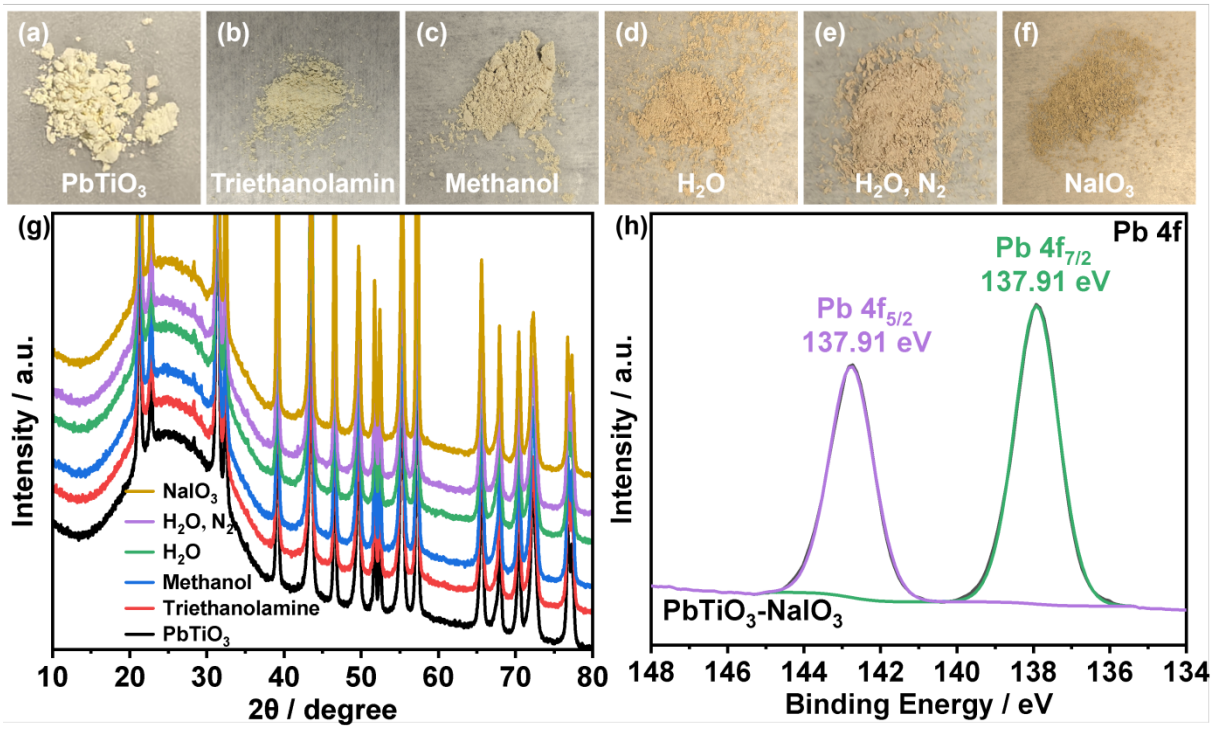

Fig. S13 $PbTiO_3$ was illuminated under various conditions with a 300 W Xe lamp. The photographs of (a) pristine $PbTiO_3$, (b) triethanolamine, (c) methanol, (d) H_2O, (e) H_2O and N_2, and (f) $NaIO_3$. (g) XRD patterns of colored $PbTiO_3$. (h) High-resolution XPS spectrum of $PbTiO_3$-$NaIO_3$ for Pb 4f.

Notably, the color of $PbTiO_3$ exhibited negligible variation in the presence of hole scavengers (triethanolamine and methanol), but turned to reddish in their absence. The XRD patterns of colored $PbTiO_3$ samples showed no obvious change, indicating that no major catalyst degradation occurred. Furthermore, in the high-resolution spectrum of Pb 4f of $PbTiO_3$-$NaIO_3$, the most strongly colored sample, two separate peaks at 142.76 and 137.91 eV were indexed to Pb $4f_{5/2}$ and Pb $4f_{7/2}$ of Pb^{2+}, respectively, conforming that Pb remained in its original state. It was speculated that the accumulated photogenerated holes induced the partial lattice distortion in $PbTiO_3$ (undetectable by XRD), thereby resulting in the color changes and the appearance of new peaks in the high-resolution in-situ XPS spectra of Pb 4f.

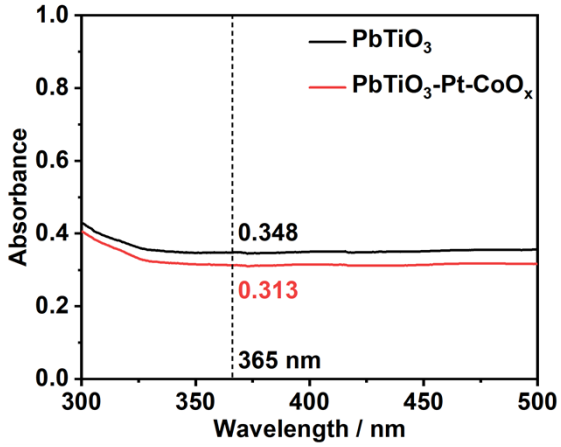

Fig. S14 The UV-Visible absorption spectra of $PbTiO_3$ and $PbTiO_3$-Pt-CoO_x photoanodes.

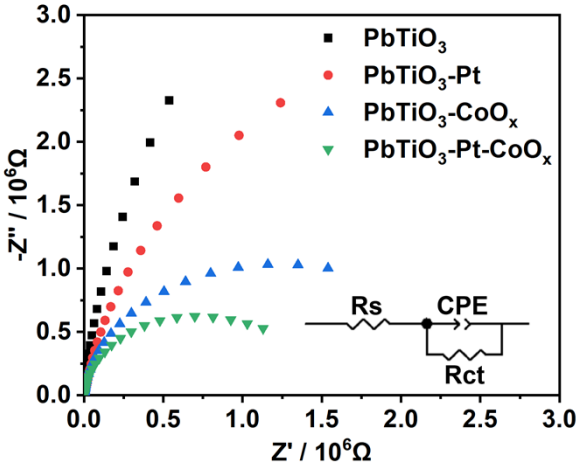

Fig. S15 EIS Nyquist plots and the corresponding equivalent circuit of $PbTiO_3$, $PbTiO_3$-Pt, $PbTiO_3$-CoO_x and $PbTiO_3$-Pt-CoO_x measured in 0.5 M Na_2SO_4 and 0.1 M benzylamine mixed aqueous solution.

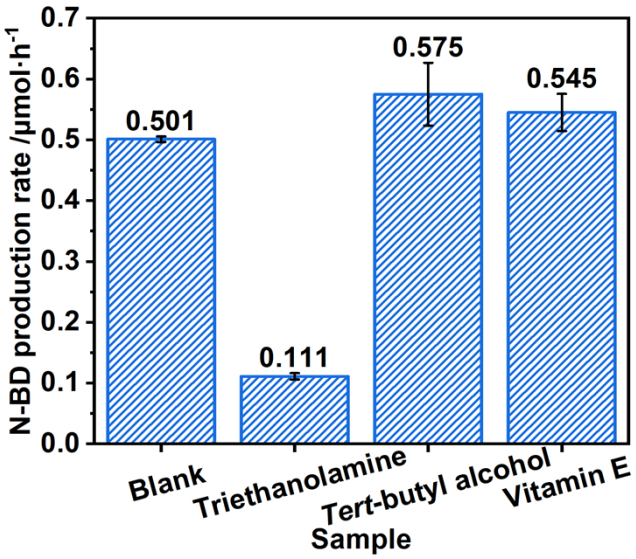

Fig. S16 Average photocatalytic BOR rates of $PbTiO_3$-Pt-CoO_x with different scavengers.

Table S1 Comparison of photocatalysts for synergistic HER-BOR dual-functional reaction.

Photocatalysts[Ref.]	**Light source**	**Reaction solution**	**Catalyst amount (mg)**	**H_2 evolution rate ($\mu mol \cdot g^{-1} \cdot h^{-1}$)**	**N-BD production rate ($\mu mol \cdot g^{-1} \cdot h^{-1}$)**
$In_{4/3}P_2Se_6$[1]	300 W Xe lamp, $\lambda > 300$ nm	20 mL acetonitrile 100 μL H_2O 0.2 mmol benzylamine	20	55.94	42.56
Pt@UiO-66-NH_2@$ZnIn_2S_4$[2]	300 W Xe lamp, $\lambda > 420$ nm	20 mL acetonitrile 500 μL H_2O 100 μL benzylamine	20	850	yield 78%
CuS/TiO_2[3]	300 W Xe lamp	40 mL DMF 500 μL H_2O 400 μL benzylamine	20	705.8	881.3
Pd_{SA+C}/TiO_2-V_O[4]	300 W Xe lamp	50 mL DMF 500 μL H_2O 500 μL benzylamine	10	585.4	257.3
Pt/PCN-777[5]	300 W Xe lamp	5 mL DMF 50 μL H_2O 50 μL benzylamine	10	332	486
This work $PbTiO_3$-Pt-CoO_x	300 W Xe lamp, AM 1.5G filter	20 mL of water-acetonitrile (60/40) mixtures 500 μL of benzylamine	10	82.97	50.10

Table S2 Fitted EIS data.

Sample	Rs (Ω)	Rct (Ω)
$PbTiO_3$	1762	2.94×10^{12}
$PbTiO_3$-Pt	28.13	1.81×10^{7}
$PbTiO_3$-CoO_x	27.01	2.23×10^{6}
$PbTiO_3$-Pt-CoO_x	27.28	1.41×10^{6}

Reference

1 B. Wu, X. Zhan, P. Yu, J. Meng, M. G. Sendeku, F. T. Dajan, N. Gao, W. Lai, Y. Yang, Z. Wang and F. Wang, *Nanoscale*, 2022, **14**, 15442-15450.

2 L. Wang, Y. Zhao, B. Zhang, G. Wu, J. Wu and H. Hou, *Catal. Sci. Technol.*, 2023, **13**, 2517-2528.

3 J. Liu, X. Sun, Y. Fan, Y. Yu, Q. Li, J. Zhou, H. Gu, K. Shi and B. Jiang, *Small*, 2024, **20**, 2306344.

4 T. Wang, X. Tao, X. Li, K. Zhang, S. Liu and B. Li, *Small*, 2021, **17**, 2006255.

5 H. Liu, C. Xu, D. Li and H. Jiang, *Angew. Chem. Int. Ed.*, 2018, **130**, 5477-5481.